Environ. Sci. Technol. **1997**, *31*, 89−95

Novel Photocatalytic Mechanisms for $CHCl_3$, $CHBr_3$, and $CCl_3CO_2^-$ Degradation and the Fate of Photogenerated Trihalomethyl Radicals on TiO_2

WONYONG CHOI† AND MICHAEL R. HOFFMANN*

W. M. Keck Laboratories, California Institute of Technology, Pasadena, California 91125

The photocatalytic degradation of $CHCl_3$, $CHBr_3$, CCl_4, and $CCl_3CO_2^-$ is investigated in aqueous TiO_2 suspensions. A common intermediate, the trihalomethyl radical, is involved in the degradation of each substrate except for $CCl_3CO_2^-$. $CHCl_3$ and $CHBr_3$ are degraded into carbon monoxide and halide ions in the absence of dissolved oxygen. The anoxic degradation proceeds through a dihalocarbene intermediate, which is produced by sequential reactions of the haloform molecule with a valence band hole and a conduction band electron. Carbon dioxide and halide ion are formed as the primary products during $CHCl_3$ degradation in the presence of oxygen. Under these conditions, the trihalomethyl radicals react rapidly with dioxygen. At pH > 11, degradation of the haloforms is enhanced dramatically. This enhancement is ascribed to *photoenhanced hydrolysis*. The secondary reactions of the trichloromethyl radical generated during CCl_4 photolysis is strongly influenced by the nature of the electron donors. Both $^{\bullet}CCl_3$ and Cl^- production increase substantially when 2-propanol is present as an electron donor. A new photocatalytic mechanism for $CCl_3CO_2^-$ degradation, which involves the formation of a dichlorocarbene intermediate, is proposed.

Introduction

Halogenated organic compounds are the most frequent and important chemical contamitants in a wide range of environments. In addition, their general toxicity raises serious concerns about their impacts on human health. The degradation of halogenated compounds is known to proceed through a series of free radical reactions. TiO_2 photocatalysis, which has been demonstrated to be effective for mineralization of a variety of organic compounds (*1*−*3*), involves the production of free radicals on the illuminated TiO_2 surface. However, our knowledge about the fate of carbon-centered radicals generated during photocatalysis is far from complete.

The reaction mechanisms in heterogeneous radical chemistry are often different from their homogeneous counterparts due to the influence of the solid surface (*4*). However, many suggested mechanisms for photocatalytic reactions are inferred from well-documented homogeneous reactions. Previous studies (*5, 6*) proposed a photocatalytic mechanism for $CHCl_3$ degradation, which was based on the reaction of trichloromethyl peroxyl radical ($Cl_3COO^{\bullet}$) whose chemistry was well understood from homogeneous radiolysis (*7*−*10*). Trichloromethyl radicals in oxygenated aqueous solutions react rapidly with dioxygen (*vide infra*, eq 3) at a rate near the diffusion limit ($k = 3.3 \times 10^9\ M^{-1}\ s^{-1}$) (*10*).

Our recent studies (*11, 12*) on the photocatalytic reduction of CCl_4, however, demonstrated that $^{\bullet}CCl_3$ on the TiO_2 surface could react not only with an oxygen molecule but also directly with a conduction-band electron (eq 4). The $^{\bullet}CCl_3$ radical can be formed on TiO_2 surface via $CHCl_3$ oxidation through valence band (VB) hole transfer (eq 1) or from CCl_4 reduction through conduction band (CB) electron transfer (eq 2). The subsequent reactions of $^{\bullet}CCl_3$ should follow similar pathways in both systems.

$$CHCl_3 + h_{vb}^+ \text{ (or } {}^{\bullet}OH) \rightarrow {}^{\bullet}CCl_3 + H^+ \text{ (or } H_2O) \quad (1)$$

$$CCl_4 + e_{cb}^- \rightarrow {}^{\bullet}CCl_3 + Cl^- \quad (2)$$

$$^{\bullet}CCl_3 + O_2 \rightarrow {}^{\bullet}OOCCl_3 \quad (3)$$

$$^{\bullet}CCl_3 + e_{cb}^- \rightarrow :CCl_2 + Cl^- \quad (4)$$

$$^{\bullet}OOCCl_3 \rightarrow \rightarrow CO_2 + 3Cl^- \quad (5)$$

$$:CCl_2 + H_2O \rightarrow CO + 2HCl \quad (6)$$

The above argument opens up the possibility for recognition of a new $CHCl_3$ degradation pathway in which there is a redox-mediated short circuiting of the VB holes and CB electrons. The new pathway could make the photocatalytic degradation of $CHCl_3$ possible in the absence of dissolved oxygen by producing CO instead of CO_2 as a final product (eq 6).

In order to test the possibility of the alternative mechanism (eqs 1, 4, and 6), the photocatalytic degradation of $CHCl_3$ is re-examined. In this work, we explore evidence for this novel photocatalytic mechanism for $CHCl_3$ and $CHBr_3$ photooxidation. Reactions of trichloromethyl radical, which are generated from the CCl_4/electron donor system, are compared to those of the $CHCl_3$ system in an attempt to ascertain the general fate of the trihalomethyl radical on illuminated TiO_2. In addition, trichloromethyl radical generation from trichloroacetate photooxidation via a photo-Kolbe process (eq 7) (*1, 13, 14*) is investigated.

$$Cl_3CCO_2^- + h_{vb}^+ \rightarrow {}^{\bullet}CCl_3 + CO_2 \quad (7)$$

Experimental Section

Materials, Apparatus, and Operation. Degussa (P25) TiO_2, which is known to be a mixture of 80% anatase and 20% rutile with an average particle size of 30 nm and BET surface area of ~50 m^2/g (*15*), was used as a photocatalyst without further treatment. All TiO_2 suspensions were prepared at a concentration of 0.5 g/L in water purified with a Milli-Q UV Plus system (resistivity, 18.2 MΩ·cm). The TiO_2 suspension was dispersed by simultaneous sonication and shaking in an ultrasonic cleaning bath (Branson 5200). The suspension was then bubbled with O_2, N_2, or a mixture (O_2/N_2) at a fixed ratio for 1 h before addition of the organic substrate. The suspension was stirred magnetically throughout each experiment. Saturated solutions of CCl_4 (5 mM), $CHCl_3$ (63 mM), and $CHBr_3$ (12 mM) were prepared by stirring in an excess of each organic liquid in water, and solutions of a desired concentration were then prepared by dilution. For anoxic (i.e., oxygen free) photodegradation experiments, separate

* To whom correspondence should be addressed; e-mail: mrh@cco.caltech.edu; phone: 818-395-4391; fax: 818-395-3170.

† Present address: Atmospheric Chemistry Element, Earth and Space Sciences Division, Jet Propulsion Laboratory, Pasadena, CA 91109.

S0013-936X(96)00157-5 CCC: $14.00

saturated stock solutions were prepared under nitrogen. Fresh stock solutions of $CHBr_3$ were made daily because of its slow hydrolytic decomposition. The pH of the suspension was adjusted with 1 N $HClO_4$ or 1 N NaOH and was measured before and after the irradiation. CCl_4 (Baker), $CHCl_3$ (Baker), CCl_3COONa (Aldrich), and $CHBr_3$ (Aldrich) were used as received.

Irradiations were performed with a 1000-W Xe arc lamp (Spindler and Hoyer) operated at 910 W. Light was filtered through a 10-cm IR water filter and, when light intensities needed to be measured, a UV band pass filter (310−400 nm, Corning). The filtered light was focused through a convex lens onto a reactor cell loaded with the TiO_2 suspension. Light intensity measurements were performed by chemical actinometry using (*E*)-α-(2,5-dimethyl-3-furylethylidene) (isopropylidene) succinic anhydride (Aberchrome 540) (*16*). A typical light intensity through a UV band pass filter was ~1.4 × 10^{-3} Einstein L^{-1} min^{-1}.

Two distinct types of photolysis experiments were carried out. One set of experiments was focused on the formation of halogenated intermediates and halide ions and the disappearance of substrate compounds as a function of irradiation time; another set was focused on the determination of gaseous CO and CO_2 generation after 2 h of irradiation. The two sets of photolysis experiments were performed in different reactors as described below.

Photolysis and Analysis of Halogenated Compounds and Halide Ions. For the experiments in which halogenated intermediates and halide ions were determined, a 35-mL quartz reactor cell was used. After gas saturation, reagents (an aliquot of the saturated stock solution and alcohols as an electron donor for CCl_4 degradation) were added into the reactor with minimal head space through a rubber septum. Light was irradiated through a UV band pass filter.

Sample aliquots were obtained with a 1-mL syringe, filtered through a 0.45-μm nylon filter, and injected into a 2.5-mL glass vial having a screwtop cap and a Teflon-faced septum. Halogenated compounds and their degradation intermediates were extracted with 0.5 mL of pentane immediately after sampling. Sample vials were stored at 4 °C in the dark up to 48 h before analysis. The degradation and formation of halogenated compounds and intermediates were followed chromatographically with a Hewlett-Packard (HP) 5880A gas chromatograph (GC) equipped with a ^{63}Ni electron capture detector and a HP-5 column (crosslinked 50% PhMe silicone, 25m × 0.32 mm × 1.05 μm). Nitrogen was used as the carrier gas. The GCs were calibrated daily with external standards (CCl_4, $CHCl_3$, $CHBr_3$, C_2Cl_4, and C_2Cl_6) and duplicate measurements were made for each sample. The formation of perbromoethylene (C_2Br_4), whose authentic standard was not available, was identified with a GC (HP 5890 II) connected to a mass selective detector (HP 5972A). The aqueous phase in the sampling vial was analyzed by ion-exchange chromatography (IC) for halide ions. The IC system was a Dionex Bio-LC system equipped with a conductivity detector and a Dionex OmniPac PAX-500 column (8 μm × 5 mm × 250 mm).

Photolysis and Analysis of Gaseous Products. The experiments determining CO and CO_2 used a Pyrex reactor with a total volume of 100 mL. The Pyrex reactor was connected to a gas collection tube (total volume 145 mL, Ace Glass) through a glass joint, which was evacuated with a closed stopcock. After N_2 or O_2 purging, 0.5 mL of $CHCl_3$ or CCl_4 was added directly into the suspension. By the end of photolysis, most of $CHCl_3$ dissolved into the aqueous suspension while excess CCl_4 droplets remained at the bottom of the reactor. A He-filled balloon was then attached to a top opening of the reactor in order to collect gaeous product evolved during the photolysis. The full band irradiation (with no filter) lasted for 2 h. At the end of each photolysis, the evacuated gas collection tube was filled with the gas mixture in the balloon and taken for GC analysis. Two aliquots of 1-mL aqueous phase were sampled, filtered, and injected into the same glass vial descibed above. In order to drive aqueous carbonate species into the gas phase (for CO_2 analysis), 100 μL of concentrated sulfuric acid was added. The vial was then shaken and left for at least 30 min for equilibration before GC analysis. Standard solutions of sodium carbonate for CO_2 analysis were prepared by the same method.

The Cl^- production after the photolysis was measured with an Orion chloride ion-selective electrode (Model 96-17B). Gaseous samples from the gas collecting tube and the head space of the glass vials were analyzed by a GC (Carle AGC series 400) equipped with a thermal conductivity detector and columns of Porapak QS and 5-Å molecular sieve particles. Helium was used as the carrier gas. Duplicate measurements were made for each sample with an injection volume of 20 μL. Standards of gaseous CO and CO_2 were made by mixing each gas with He at known ratios in the gas collecting tube. The total numbers of CO and CO_2 molecules generated during the photolysis were calculated by using Henry's law constants based on the assumption of liquid−gas equilibrium.

Results

Results of the photocatalytic degradations of $CHCl_3$ and $CHBr_3$ under N_2 saturation are shown in Figure 1. Even though dioxygen was considered to be essential for the degradation of these compounds (*5* ,*6, 17, 18*), they were decomposed slowly in the N_2-saturated photocatalytic systems. The linearity of halide production over the whole irradiation period indicates that the contribution from the residual oxygen, which remains even after vigorous N_2 purging, to total halide production is insignificant. In particular, the degradation rates were greatly enhanced at pH 12 for both $CHCl_3$ and $CHBr_3$. Although $CHCl_3$ and $CHBr_3$ can be degraded through base-catalyzed hydrolysis (eqs 8−10) in the absence of light (*19, 20*), the hydrolysis rate at pH 12 is small compared to the net photolysis rate as shown in Figure 1.

$$CHX_3 + OH^- \rightarrow CX_3^- + H_2O \ (X = Cl^- \text{ or } Br^-) \quad (8)$$

$$CX_3^- \leftrightarrow :CX_2 + X^- \quad (9)$$

$$:CX_2 + H_2O \rightarrow CO + 2H^+ + 2X^- \quad (10)$$

The measured quantum yields for the halide production were $\Phi_{CHCl_3} = 0.021$ ($CHCl_3$ at pH 12), $\Phi_{CHCl_3} = 0.0034$ ($CHCl_3$ at pH 5), $\Phi_{CHBr_3} = 0.018$ ($CHBr_3$ at pH 12), and $\Phi_{CHBr_3} = 0.0019$ ($CHBr_3$ at pH 5).

The effects of the dissolved oxygen concentration on the photolysis rate of $CHCl_3$ are shown in Figure 2. These results show that O_2 increases the net dechlorination rate. The stoichiometry for the complete mineralization of $CHCl_3$ to CO_2 in the presence of oxygen is (*5, 17*)

$$CHCl_3 + H_2O + {}^1/_2O_2 \rightarrow CO_2(g) + 3HCl(aq) \qquad \Delta H_{298} = -113.1 \text{ kcal/mol} \quad (11)$$

For $CHCl_3$ photodegradation in an air-saturated solution (Figure 2a), the Cl^- production, however, went beyond the level of concentration that corresponded to the stoichiometric consumption of dissolved O_2. This result is not consistent with the observations of Kormann et al. (*5*). They observed that [Cl^-] increased linearly up to ~1.4 mM, at which point the chloride production rate abruptly decreased to a much smaller value as the O_2 was depleted.

The normal effect of [O_2] on the dechlorination rate (Figure 2b) exhibited Langmurian dependence (*21, 22*) except that

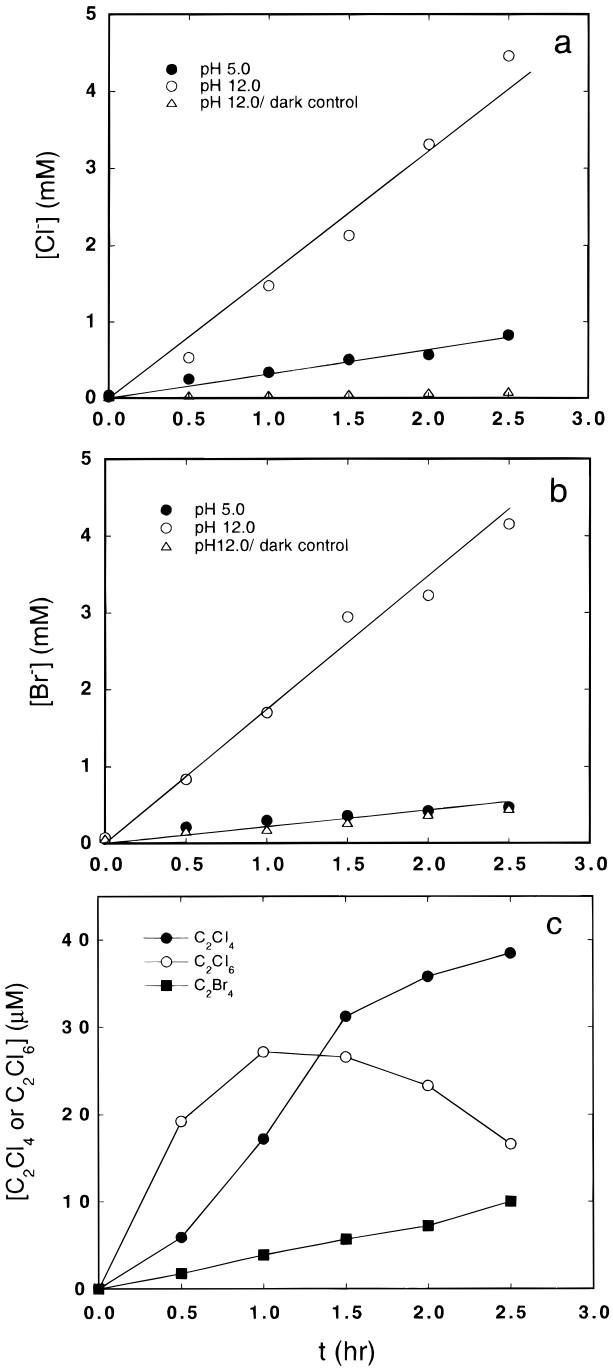

FIGURE 1. Production of halide ions from the photocatalytic decomposition of (a) 6 mM $CHCl_3$ and (b) 6 mM $CHBr_3$ and (c) the production of halogenated byproducts at pH 12 (C_2Cl_4 and C_2Cl_6 from 6 mM $CHCl_3$ solution and C_2Br_4 from 6 mM $CHBr_3$ solution) as a function of irradiation time. Suspensions were saturated with N_2 prior to the photolysis in a sealed reactor at the initial pH 5 or pH 12. The halide generations from dark hydrolysis of the same substrates at pH 12 are shown as well. There was no hydrolysis at pH 5. The concentration of C_2Br_4 in panel c could not be quantified since its authentic sample was not available.

the dechlorination rate was non-zero at $[O_2] = 0.0$ mM. The data of Figure 3 are fitted to

$$\frac{d[Cl^-]}{dt} = k_{Cl}\frac{K_{O_2}[O_2]}{1 + K_{O_2}[O_2]} + k_{Cl,0} \qquad (12)$$

where k_{Cl} is a photodechlorination rate constant in the presence of dissolved oxygen, K_{O_2} is a photochemical equivalent of O_2 adsorption constant, and $k_{Cl,0}$ is a photodechlorination rate in the absence of dissolved oxygen. The fitted values were $k_{Cl} = 11.5\ \mu M\ min^{-1}$, $K_{O_2} = 3.4 \times 10^3\ M^{-1}$ and $k_{Cl,0} = 3.4\ \mu M\ min^{-1}$. Mills et al. (*23*) reported a value of $K_{O_2} = 3.6 \times 10^3\ M^{-1}$ in a TiO_2 (Degussa P25)/ 4-chlorophenol system while Okamoto et al. (*24*) obtained $K_{O_2} = 8.9 \times 10^3\ M^{-1}$ in a TiO_2 (anatase)/phenol system. However, a value of $K_{O_2} = (1.3 \pm 0.7) \times 10^5\ M^{-1}$, which Kormann et al. (*5*) reported for a TiO_2 (Degussa P25)/chloroform system, appears to be an overestimate.

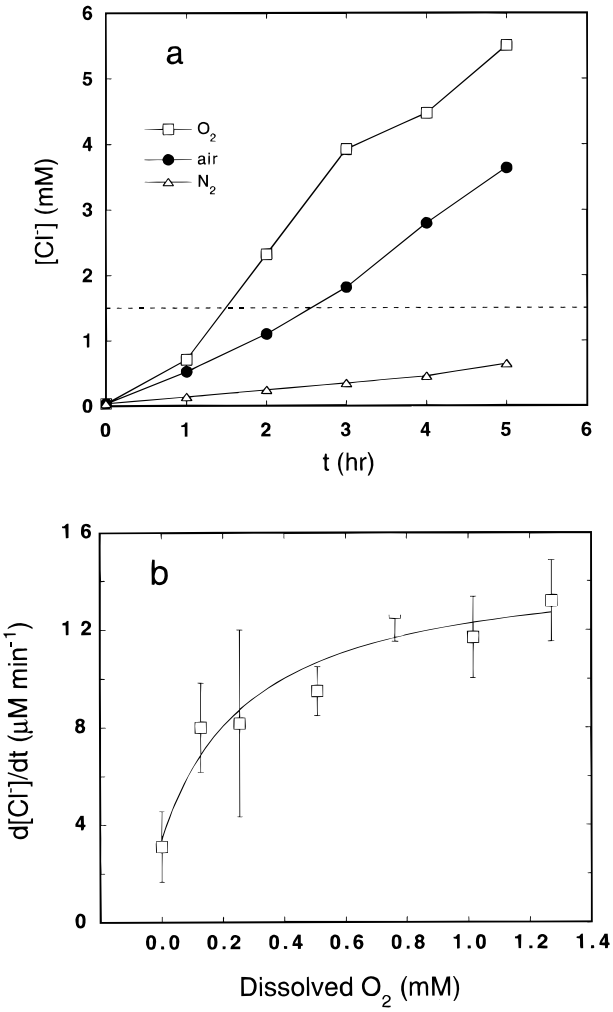

FIGURE 2. (a) Chloride generation from the photolysis of 6 mM $CHCl_3$ solutions (pH_i 4.5) that were saturated with O_2, air, and N_2, respectively, prior to irradiation. The dotted line represents the chloride level corresponding to the stoichiometric consumption of dissolved oxygen (0.25 mM) in an air-saturated solution. (b) Dependence of the photocatalytic chloride generation rates in 6 mM $CHCl_3$ solution on the dissolved oxygen concentration. The dechlorination rates were measured over an initial 1-h photolysis period. The concentration of dissolved oxygen was varied by changing the ratio of the flow rates of O_2 and N_2 bubbling gases and calculated by assuming that the dissolved oxygen concentration in an O_2-saturated solution was 1.27 mM. The solid line is a fit to eq 12.

The pH-dependent dechlorination rates and formation of intermediates during $CHCl_3$ degradation are compared between O_2- and N_2-saturated suspensions in Figure 3. Production of Cl^- in O_2-saturated solutions increased exponentially at pH > 10, while the N_2-saturated systems showed a moderate increase in $[Cl^-]$. The calculated hydrolysis (*25*) of $CHCl_3$ as a function of pH (dotted line in Figure 3a) shows that the Cl^- production from hydrolysis was about 100−1000 times smaller than that due to photolysis. The formation of C_2Cl_6 and C_2Cl_4 (Figure 3b) was only significant at pH > 11.5,

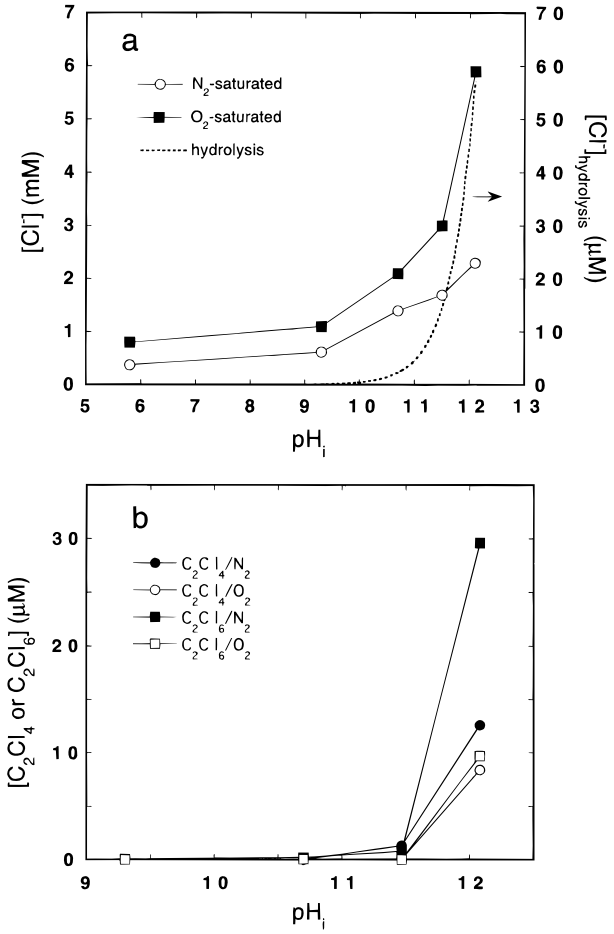

FIGURE 3. Effect of the initial pH of TiO_2 suspension on the photocatalytic production of (a) chloride and (b) C_2Cl_4 and C_2Cl_6 in 6 mM $CHCl_3$ solutions, which were saturated with O_2 or N_2 prior to irradiation. Concentrations were measured after 1-h irradiation. The dotted line in panel a represents calculated pH-dependent chloride production after 1-h dark hydrolysis.

and their concentrations were higher in N_2-saturated solutions than in O_2-saturated solutions.

Due to the high substrate concentration (6 mM) used in this study, dimerization products of the intermediate radicals were detected (eqs 13−15).

$$2^{\bullet}CCl_3 \rightarrow Cl_3CCCl_3 \quad (13)$$

$$2{:}CCl_2 \rightarrow Cl_2C{=}CCl_2 \quad (14)$$

$$2{:}CBr_2 \rightarrow Br_2C{=}CBr_2 \quad (15)$$

The time-dependent production of the dimerized products from $CHCl_3$ and $CHBr_3$ degradation at pH 12 are shown in Figure 1c. Both C_2Cl_6 and C_2Cl_4 from $CHCl_3$ degradation were detected as byproducts while only C_2Br_4 (not C_2Br_6) was detected from $CHBr_3$ degradation. The concentration of C_2Cl_6 reached its maximum in 1 h. The concentrations of C_2Cl_4 and C_2Br_4 rose continuously. In control reactions, which were performed in the dark, a trace amount of C_2Br_4 and 0.2 μM C_2Cl_4 were formed after 2.5 h from a dimerization of hydrolytically produced dihalocarbenes (eqs 8 and 9).

In order to examine the possibility of trichloromethyl radical production during trichloroacetate photooxidation (eq 7), C_2Cl_6 and C_2Cl_4 were sought as byproducts from the photolysis of trichloroacetate on TiO_2. No C_2Cl_6 was detected throughout the photolysis runs listed in Table 1. However, a trace of C_2Cl_4 was found in some cases. Few differences in the dechlorination rates were found under O_2 and N_2; this observation is consistent to those of Chemseddine and Boehm (*14*). The dechlorination rates increased gradually with lowering pH.

TABLE 1. Chloride Production (μM) after 1-h Photolysis[a] of 6 mM Trichloroacetate Solution on TiO_2 as a Function of pH

pH	2.1	3.0	5.8	12.1
O_2-saturated	870	700	520	400
N_2-saturated	840	680	740	420

[a] Light illumination through an IR water filter and a UV band pass filter onto a 35-mL quartz reactor with an intensity of 1.4×10^{-3} Einstein L^{-1} min^{-1}.

In our previous study (*11*), we reported that the photoreductive decomposition of CCl_4 on TiO_2 was strongly dependent on the nature of the electron donors. In order to investigate how the electron donor affects the fate of trichloromethyl radical (generated through eq 2) on TiO_2, the production of chloride and chlorinated byproducts ($CHCl_3$, C_2Cl_6, and C_2Cl_4), which are derived from the trichloromethyl radical, were measured in the CCl_4/electron donor system and summarized in Table 2. The chlorinated byproduct formation varied greatly as a function of the specific electron donor. The addition of 2-propanol resulted in enhanced concentration of byproducts, while methanol showed a moderate effect. *tert*-Butanol had little effect.

The production of CO_2, CO, and Cl^- from the photolysis of $CHCl_3$ is compared in Table 3. CO was found as the main product of chloroform photolysis in the absence of O_2 and at high pH. At pH < 11 and in the absence of dissolved oxygen, $CHCl_3$ degradation was slow. In O_2-saturated suspensions, on the other hand, CO_2 was determined to be the principle product and CO was the minor product even at high pH. At low pH under N_2-saturation, the analytical method was not accurate and sensitive enough to distinguish between background CO_2 and photogenerated CO_2 and CO. The stoichiometric balance between Cl^- and gaseous products was reasonable. However, the Cl^- level was consistently a little higher than the sum of CO and CO_2; this result suggests the presence of other byproducts.

Similar analyses for CCl_4 are presented in Table 4. Both CO and CO_2 were detected as photolysis products. In addition, photolysis of the added electron donors in the absence of CCl_4 did not produce detectable levels of CO. Therefore, CO appears to have originated directly from CCl_4 degradation. Even though the chloride production under O_2 saturation was about doubled from that under N_2 saturation, CO_2 generation was enhanced more substantially in the O_2-saturated system. Based on this observation, it appears that the majority of evolved CO_2 originated from the electron donor oxidation and not from CCl_4 reduction. The sum of total CO and an undetermined fraction of total CO_2 (which came from CCl_4) accounts for only a small fraction of total Cl^-. In the present photolysis system, where excess CCl_4 droplets remained at the bottom of reactor, most of chlorinated radical intermediates seemed to react with the electron donor or to be scavenged into the CCl_4 liquid phase, thus preventing their subsequent degradation.

Discussion

Experimental results presented above clearly show that $CHCl_3$ and $CHBr_3$ are photocatalytically degraded into CO in the absence of dissolved oxygen. These results are consistent with a "short-circuit" mechanism that involves reactions of $CHCl_3$ with a VB hole (or $^{\bullet}OH$) (eq 1) and a CB electron (eq 4). The overall stoichiometry for this degradation pathway can be written as

$$CHCl_3 + H_2O \rightarrow CO(g) + 3HCl(aq) \qquad \Delta H_{298} = -45.6 \text{ kcal/mol} \quad (16)$$

TABLE 2. Concentrations of Cl^-, C_2Cl_6, and C_2Cl_4 Produced after 1-h Photolysis[a] of 1 mM CCl_4 in Air-Equilibrated TiO_2 Suspensions in the Presence of *tert*-Butanol (t-BuOH), 2-Propanol (2-PrOH), and Methanol as Electron Donors

	pH[b] 2.7				pH 5				pH 12			
	Cl^- (mM)	$CHCl_3$ (μM)	C_2Cl_6 (μM)	C_2Cl_4 (μM)	Cl^- (mM)	$CHCl_3$ (μM)	C_2Cl_6 (μM)	C_2Cl_4 (μM)	Cl^- (mM)	$CHCl_3$ (μM)	C_2Cl_6 (μM)	C_2Cl_4 (μM)
no added alcohol	0.02	nd[c]	trace[d]	nd	0.03	nd	trace	nd	0.09	nd	trace	nd
0.1 M t-BuOH	0.22	nd	trace	nd	0.17	2.2	trace	nd	0.81	nd	trace	trace
0.1 M 2-PrOH	1.9	51.3	0.51	9.1	2.2	75.1	0.56	20.1	2.5	20.6	trace	7.5
0.1 M CH_3OH	0.04	4.7	0.08	0.56	0.14	1.2	0.08	0.34	2.1	4.4	trace	9.9

[a] Light illumination through an IR water filter and a UV-band pass filter onto a 35 mL quartz reactor with an intensity of 1.4×10^{-3} Einstein L^{-1} min^{-1}. [b] Initial pH before irradiation. [c] nc, not detected. [d] Trace amount <30 nM.

TABLE 3. CO_2, CO, and Cl^- Generation after 2-h Photolysis[a] of $CHCl_3$ on TiO_2

pH/ saturated gas	N_{CO_2} (μmol)	N_{CO} (μmol)	N_{Cl^-} (μmol)/3[c]	$N_{CO_2} + N_{CO}$ (μmol)
(12.2, 11.9)[b]/N_2	3	149	187	152
(12.2, 11.6)/O_2	160	12	187	172
(12.2, 12.2)/no light	3	9	17	12
(11.9, 11.6)/N_2	3	56	97	59
(11.9, 10.3)/O_2	162	3	163	165
(11.4, 10.9)/N_2	1	11	25	12
(11.4, 3.2)/O_2	49	nd[d]	90	49
(10.2, 8.6)/N_2	1	nd	4	1
(10.2, 2.7)/O_2	52	nd	60	52
(5.0, 4.1)/N_2	1	nd	2	1
(5.0, 2.7)/O_2	41	nd	47	41

[a] Light illumination through an IR water filter only onto a 100 mL Pyrex reactor; $[TiO_2] = 0.5$ g/L in the presence of near saturated $CHCl_3$ (0.5 mL/100 mL) in the reactor. [b] The first and second numbers in the parentheses are the pH of the suspension before and after the photolysis, respectively. [c] The numbers of chloride ions are divided by 3 to make them equivalent to those of CO_2 and CO on per $CHCl_3$ molecule basis. [d] nd, not detected within the sensitivity limit of this experiment.

TABLE 4. CO_2, CO, and Cl^- Generation after 2-h of Photolysis[a] of CCl_4 on TiO_2 with *tert*-Butanol (t-BuOH) or 2-Propanol (2-PrOH) Present as Electron Donors

pH[b]/gas/electron donor[c]	N_{CO_2} (μmol)	N_{CO} (μmol)	N_{Cl^-} (μmol)/4[d]
12.2/N_2/t-BuOH	4	4	25
12.2/O_2/t-BuOH	33	1	38
12.2/N_2/2-PrOH	1	11	58
12.2/O_2/2-PrOH	86	3	115
5.0/N_2/2-PrOH	1	1	9
5.0/O_2/2-PrOH	36	nd	48

[a] Light illumination through an IR water filter only onto a 100 mL Pyrex reactor; $[TiO_2] = 0.5$ g/L in the presence of excess liquid CCl_4 (0.5 mL) in the reactor. [b] Initial pH of the suspension before the light illumination. [c] The electron donor concentration for each experiment was 0.1 M. [d] The numbers of chloride ions are divided by 4 to make them equivalent to those of CO_2 and CO on per CCl_4 molecule basis.

However, this reaction (eq 16) is preferred thermodynamically only under anoxic conditions. In O_2-saturated suspensions, most of the $^{\bullet}CCl_3$ radicals react with O_2 (eq 3) to produce CO_2 as suggested previously (*5, 8*). Therefore, the heterogeneously photogenerated trichloromethyl radical exhibits two branching pathways; the branching ratio is dependent on the availability of dioxygen on the surface.

Even though both pathways involving the trichloromethyl radical lead to the full degradation of $CHCl_3$, several experimental observations can not be readily explained by these alternative mechanisms. For example, the $CHCl_3$ dechlorination rates (Figure 3a) increase rapidly at pH > 10 in O_2-saturated suspensions while $d[Cl^-]/dt$ rises slowly in N_2-saturated suspensions. Similar behavior was reported for the kinetics of CCl_4 dechlorination on TiO_2 (*11, 12*). In that case, the enhanced rates were attributed to an increase in the rate of CB electron transfer and the base-catalyzed hydrolysis of dichlorocarbene. The same general arguments can be applied to the reactions of eqs 4 and 6. However, there is no reason why these effects should be enhanced in O_2-saturated suspensions. In addition, CO_2 production (Table 3) in the presence of O_2 was enhanced significantly at high pH. Furthermore, the rates of formation of C_2Cl_6 and C_2Cl_4 (Figure 3b) also show drastic increases above pH 11. However, during CCl_4 photoreduction the same byproducts were shown to decrease at high pH (*11, 12*). This trend is supported by the data presented in Table 2.

In order to account for these observations, a third mechanistic pathway for $CHCl_3$ and $CHBr_3$ degradation is proposed. Even though the base-catalyzed hydrolyses of the haloforms (eqs 8−10) are much slower than the corresponding photolysis rates (Figures 1 and 3a), they do increase exponentially with pH. The rate-determining steps in the hydrolyses involve the release of a halide ion from a trihalocarbanion (eq 9) (*19*). On the photoilluminated TiO_2 surface, however, an alternative pathway for a trihalocarbanion is possible as follows.

$$CX_3^- + h_{vb}^+ \rightarrow {}^{\bullet}CX_3 \qquad (17)$$

The observed polarographic cathodic wave of trichloromethyl radical ($^{\bullet}CCl_3 + e^- \rightarrow CCl_3^-$) has a half-wave potential of $E_{1/2} \approx 0.0$ V (vs NHE) (*26*). Since the VB hole potential of TiO_2 (at pH 7) is +2.7 V, there is a large thermodynamic driving force for the reaction of eq 17. When O_2 is present, the $^{\bullet}CX_3$ radical is rapidly scavenged via eqs 3 and 5. As a consequence, the equilibrium deprotonation step (eq 8) is shifted to the right. This, in turn, results in an increase in the rates of $CHCl_3$ degradation and byproduct formation with increasing pH. In the absence of O_2, the $^{\bullet}CX_3$ radical reacts with a CB electron to form $:CX_2$ (eq 4); this pathway is consistent with the slower increase of Cl^- production in N_2-saturated systems as shown in Figure 3a. Since the above phenomenon is closely related to the net effects of base-catalyzed hydrolysis, we name the process "photoenhanced hydrolysis".

The proposed photocatalytic mechanisms for $CHCl_3$ and $CHBr_3$ degradation on TiO_2 are summarized in Figure 4. The mechanism of Figure 4a represents photooxidation in the presence of dissolved oxygen, as proposed by Kormann et al. (*5*). This mechanism is the major pathway for a haloform degradation under normal conditions in which oxygen is present and hydrolysis is negligible (pH < 10). The mechanism of Figure 4b becomes a major contributor under anoxic conditions. The rate of this reaction in the absence of oxygen is much slower than that achieved in pathway a because there is no efficient CB electron scavengers available except for the transient, trihalomethyl radicals. When a sufficient amount of oxygen is present at the TiO_2 surface, the mechanisms of Figure 4, panels a and b, proceed concurrently. The experimental observation (Figure 2a) that Cl^- generation in an air-saturated TiO_2 suspension was linear beyond the stoichiometric consumption of O_2 supports this argument.

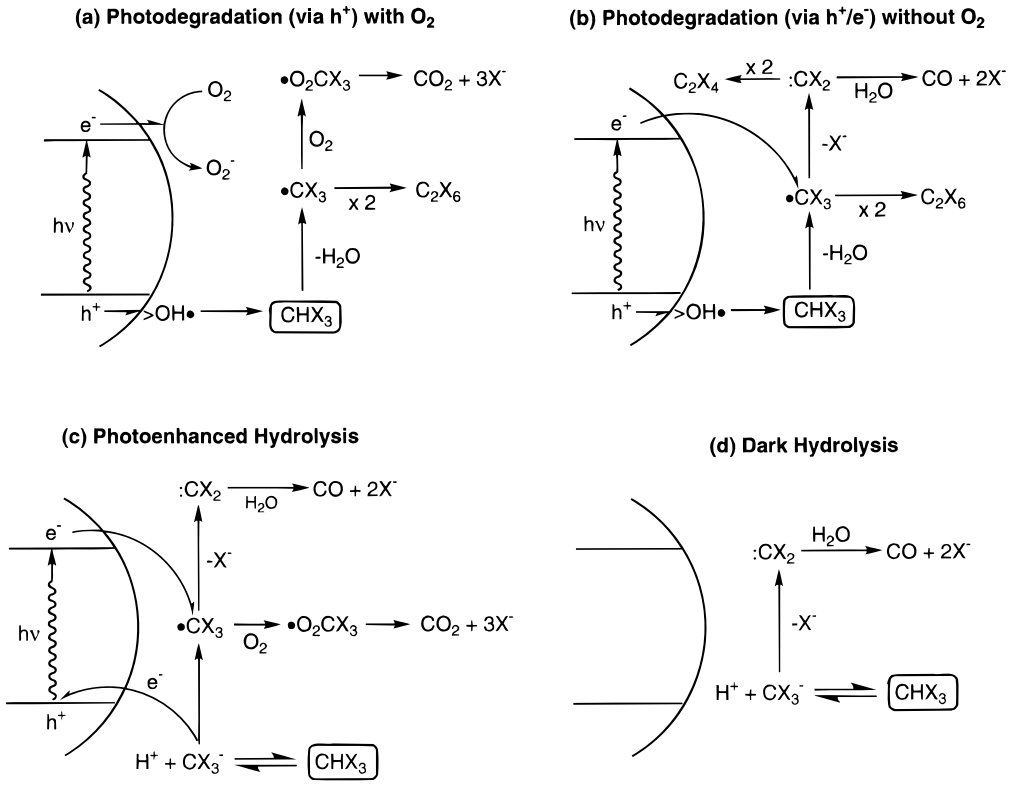

FIGURE 4. Three proposed photocatalytic mechanisms of CHX_3 (X = Cl or Br) degradation on TiO_2 and a dark hydrolysis reaction are illustratively compared.

At higher pH, the rate of dehalogenation can be increased due to enhancement in both the CB electron-transfer pathway and dihalocarbene hydrolysis. The mechanism of Figure 4c becomes important only when deprotonation of the haloform (eq 8) occurs at pH > 10. When oxygen is present, the acceleration of the degradation rate is dramatic. Without oxygen, the degradation pathway is similar to the mechanism of Figure 4b. However, at this time, it is not clear how much of the net anoxic degradation can be attributed to mechanisms b and c, respectively. The intrinsic hydrolysis pathway of Figure 4d is insignificant under the conditions employed in this study.

In contrast to the $CHCl_3$ system, the trichloromethyl radical in CCl_4 photoreduction appears only in the presence of appropriate electron donors. Since the electron donors (ROH) scavenge VB holes efficiently and induce secondary reactions through the formation of α-hydroxyalkyl radicals (*11, 27, 28*), the chemistry of $^{\bullet}CCl_3$ with efficient electron donors is substantially different from that of $^{\bullet}CCl_3$ radical generated without electron donors. As shown in Table 2, the specific electron donors have a strong influence on the production of Cl^- and chlorinated byproducts. The relative effect of a wide range of electron donors on CCl_4 dechlorination has been discussed previously (*11*).

The rates of formation of chlorinated hydrocarbon byproducts and Cl^- are enhanced substantially when 2-propanol is employed as an electron donor (Table 2). This effect can be explained by the following chain propagation steps:

$$^{\bullet}CCl_3 + (CH_3)_2CHOH \rightarrow CHCl_3 + (CH_3)_2\dot{C}OH \quad (18)$$

$$CCl_4 + (CH_3)_2\dot{C}OH \rightarrow {}^{\bullet}CCl_3 + (CH_3)_2CO + HCl \quad (19)$$

Considering the bond strength of $H-C(CH_3)_2OH$ (91 ± 1 kcal/mol) and $H-CCl_3$ (94 ± 1 kcal/mol) (*29*), this chain propagation sequence reaction is energetically feasible. With methanol C−H bond strength of 94 ± 2 kcal/mol, the chain propagation of eqs 18 and 19 should be less efficient as seen experimentally. The chain propagation of eqs 18 and 19 is inoperative in the CCl_4/*tert*-butanol system because *tert*-butanol does not form α-hydroxyalkyl radicals. The extent of chain propagation in our study seems to be limited due to the competition from O_2 addition to the carbon-centered radicals.

The net production of C_2Cl_6 in the CCl_4/ROH systems is less than that of C_2Cl_4 while the $CHCl_3$ system showed the opposite trend. At pH 12, only traces of C_2Cl_6 were found (Table 2) in contrast to its dramatic increase in the $CHCl_3$ system at the same pH (Figure 3b). This behavior is consistent with the following secondary reaction induced by the electron donor (eq 20) (*27*).

$$RR'\dot{C}OH + {}^{\bullet}CCl_3 \rightarrow RR'CO + :CCl_2 + HCl \quad (20)$$

The oxidation potentials of $^{\bullet}CH_2OH$ (−0.74 V vs NHE) and $^{\bullet}C(OH)(CH_3)_2$ (−1.06 V) (*27*) are strong enough to directly reduce $^{\bullet}CCl_3$ (0.0 V). The reduced surface concentration of $^{\bullet}CCl_3$ results in fewer net dimerizations to produce C_2Cl_6 while at the same time $:CCl_2$ dimerization to produce C_2Cl_4 is enhanced.

In general, photocatalytic degradation of organic compounds on illuminated TiO_2 is thought to be initiated through hydrogen atom abstraction by surface-bound $^{\bullet}OH$ radical (*13, 14*). Therefore, organic compounds having no abstractable hydrogen atoms such as CCl_4 and $CCl_3CO_2^-$ exhibit much slower overall degradation rates (*13, 14, 18, 30*). In the case of $CCl_3CO_2^-$, the slow degradation rates were attributed to either the photo-Kolbe reaction (eq 7) (*1, 3, 14*) and/or the photoreduction by CB electrons (eq 21) (*14, 31*), although it was not clear which was the predominant pathway mechanism.

$$CCl_3CO_2^- + e_{cb}^- \rightarrow {}^{\bullet}CCl_2CO_2^- + Cl^- \quad (21)$$

Supporting evidence for the photo-Kolbe mechanism is that CO_2 is formed from trichloroacetate degradation in N_2-

saturated TiO_2 suspensions (*14*). On the other hand, Chemseddine and Boehm (*14*) reported that CO_2 production under N_2 decreased in the order of $CCl_3CO_2^- > CHCl_2CO_2^- > CH_2ClCO_2^- > CH_3CO_2^-$, which is consistent with a reaction initiated by CB electrons. We should expect the opposite order if the photo-Kolbe mechanism is working because electron density at the carboxyl group is decreasing with an increasing number of chlorine atoms. In this study, we did not detect C_2Cl_6 from the fairly concentrated solution (6 mM) of trichloroacetate, even though it was formed during the photodegradation of $CHCl_3$ and CCl_4.

In order to resolve this mechanistic dilemma, we propose the following photocatalytic mechanism of trichloroacetate degradation, which is initiated by eq 21 and then followed by eqs 22 and 23.

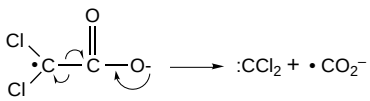

(22)

$$\bullet CO_2^- + h_{vb}^+ \longrightarrow CO_2 \qquad (23)$$

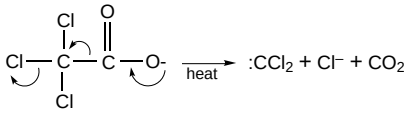

(24)

A similar thermolytic decarboxylation mechanism (eq 24) of trichloroacetate is known (*20*). In agreement with our mechanism proposed above, Mao et al. (*13*) detected oxalate as a minor product from the photocatalytic degradation of trichloroacetate. The oxalate molecule can be formed from the dimerization of $^{\bullet}CO_2^-$ radicals. Since the carboxyl group of the trichloroacetate molecule has a very low electron density due to the presence of three electron-withdrawing substitutes, decarboxylation appears to result from self-rearrangement (eq 22) rather than from the direct photo-Kolbe reaction. Additional study of the trichloroacetate photodegradation on TiO_2 is needed in order to verify the proposed mechanism.

Acknowledgments

We thank the Advanced Research Projects Agency (ARPA) and the Office of Naval Research (ONR) {N0014-92-J-1901} for financial support. We also appreciate the help from Robert Rossi and Janet Kesselman in GC analysis.

Literature Cited

(1) Hoffmann, M. R.; Martin, S. T.; Choi, W.; Bahnemann, D. W. *Chem. Rev.* **1995**, *95*, 69.
(2) Serpone, N., Pelizzetti, E., Eds. *Photocatalysis—Fundamentals and Applications;* Wiley-Interscience: New York, 1989.
(3) Ollis, D. F., Al-Ekabi, H., Eds. *Photocatalytic Purification and Treatment of Water and Air;* Elsevier: Amsterdam, 1993.
(4) Mao, Y.; Schöneich, C.; Asmus, K.-D. *J. Phys. Chem.* **1992**, *96*, 8522.
(5) Kormann, C.; Bahnemann, D. W.; Hoffmann, M. R. *Environ. Sci. Technol.* **1991**, *25*, 494.
(6) Bahnemann, D.; Bockelmann, D.; Goslich, R. *Solar Energy Mater.* **1991**, *24*, 564.
(7) Köster, R.; Asmus, K.-D. Z. *Naturforsch.* **1971**, *26B*, 1108.
(8) Mönig, J.; Bahnemann, D.; Asmus, K.-D. *Chem.—Biol. Interact.* **1983**, *45*, 15.
(9) Mönig, J.; Asmus, K.-D. *J. Chem. Soc. Perkin Trans. 2* **1984**, 2057.
(10) Lal, M.; Schöneich, C.; Mönig, J.; Asmus, K.-D. *Int. J. Radiat. Biol.* **1988**, *54*, 773.
(11) Choi, W.; Hoffmann, M. R. *Environ. Sci. Technol.* **1995**, *29*, 1646.
(12) Choi, W.; Hoffmann, M. R. *J. Phys. Chem.* **1996**, *100*, 2161.
(13) Mao, Y.; Schöneich, C.; Asmus, K.-D. *J. Phys. Chem.* **1991**, *95*, 10080.
(14) Chemseddine, A.; Boehm, H. P. *J. Mol. Catal.* **1990**, *60*, 295.
(15) *Degussa Technical Bulletin Pigments* No. 56; Degussa: Hanau-Wolfgang, 1990.
(16) Heller, H. G.; Langan, J. R. *J. Chem. Soc., Perkin Trans. 2* **1981**, 341.
(17) Pruden, A. L.; Ollis, D. F. *Environ. Sci. Technol.* **1983**, *17*, 628.
(18) Hsiao, C.-Y.; Lee, C.-L.; Ollis, D. F. *J. Catal.* **1983**, *82*, 418.
(19) Robinson, E. A. *J. Chem. Soc.* **1961**, 1663.
(20) March, J. *Advanced Organic Chemistry*, 3rd ed.; John Wiley & Sons: New York, 1985.
(21) Pelizzetti, E.; Pramuro, E.; Minero, C.; Serpone, N.; Borgadello, E. In *Photocatalysis and Environment;* Schiavello, M., Ed.; NATO ASI Series; Kluwer Academic Publication: Dordrecht, The Netherlands, 1988; p 527.
(22) Al-Ekabi, H.; Serpone, N.; Pelizzetti, E.; Minero, C.; Fox, M. A.; Draper, R.B. *Langmuir* **1989**, *5*, 250.
(23) Mills, A.; Morris, S. *J. Photochem. Photobiol. A: Chem.* **1993**, *71*, 75.
(24) Okamoto, K.-I.; Yamamoto, Y.; Tanaka, H.; Itaya, A. *Bull. Chem. Soc. Jpn.* **1985**, *58*, 2023.
(25) The hydrolysis rate constant was taken from Schwarzenbach, R. P.; Gschwend, P. M.; Imboden, D. M. *Environmental Organic Chemistry;* John Wiley & Sons: New York, 1993; p 368.
(26) Bansal, K. M.; Henglein, A.; Sellers, R. M. *Ber. Bunsen-Ges. Phys. Chem.* **1974**, *78*, 569.
(27) Lilie, V. J.; Beck, G.; Henglein, A. *Ber. Bunsen-Ges. Phys. Chem.* **1971**, *75*, 458.
(28) Ross, A. B.; Neta, P. *Rate Constants for Reactions of Aliphatic Carbon-Centered Radicals in Aqueous Solution;* NSRDS-NBS 70; National Bureau of Standards: Washington, DC, 1982.
(29) *CRC Handbook of Chemistry and Physics*, 74th ed.; CRC Press: Boca Raton, FL, 1993.
(30) Ollis D. F.; Hsiao, C.-Y.; Budiman, L.; Lee, C.-L. *J. Catal.* **1984**, *88*, 89.
(31) The half-wave potential of trichloroacetate reduction is −0.49 V (vs NHE), which is comparable to TiO_2 CB electron potential (−0.5 V at pH 7); The half-wave potential was taken from Meites, T.; Meites, L. *Anal. Chem.* **1955**, *27*, 1531.

Received for review February 20, 1996. Revised manuscript received August 16, 1996. Accepted August 26, 1996.[⊗]

ES960157K

[⊗] Abstract published in *Advance ACS Abstracts*, November 1, 1996.